J Mater Sci (2010) 45:2862–2867
DOI 10.1007/s10853-010-4275-0

Magnetically recyclable hollow Co–B nanospindles as catalysts for hydrogen generation from ammonia borane

**D. G. Tong · X. L. Zeng · W. Chu ·
D. Wang · P. Wu**

Received: 12 October 2009 / Accepted: 22 January 2010 / Published online: 6 February 2010

Abstract Magnetically recyclable Co–B hollow nanospindles have been prepared by using poly(styrene-*co*-methacrylic acid) nanospindles as scarified templates for the first time. The effect of the weight ratio of poly(styrene-*co*-methacrylic acid) to $Co(OAc)_2$ on the structure of Co–B hollow nanospindles is not significant. In the hydrolysis of ammonia borane to release H_2, the activity of Co–B hollow nanospindles was much higher than that of regular Co–B prepared without templates. Their catalytic performance is comparable to that of the reported Pt black concerning hydrogen yield. The favorable activity is attributed to the large specific surface area and hollow structure. In addition, Co–B hollow nanospindles have good reusability in the application due to their unique magnetic properties.

Introduction

Hydrogen is gaining a great deal of attention as an energy carrier as well as an alternative fuel [1]. In past decades, various kinds of materials for hydrogen storage have been investigated. Typical examples are AB_5-type electrode alloys, metal/complex hydrides, metal nitrides and imides, carbon materials, inorganic nanostructures, and metal–organic frameworks [1–6]. Recently, ammonia borane (NH_3BH_3) has been paid considerable research attention as a promising new entry to the hydrogen storage materials [6–9]. Xu et al. [7, 9] reported a high-performance hydrogen generation system based on transition metal-catalyzed hydrolysis of NH_3BH_3 at room temperature. However, for practical use, the development of low-cost and highly efficient catalysts is desired.

Co–B materials have attracted much attention due to their unique performance and low-cost in the catalytic field [10–17]. In view of the literatures, the microstructures and surface morphologies of the Co–B play a crucial role in the catalytic performance [11–17]. Recently, Tong et al. [13, 14] described that the mesoporous and flower-like Co–B exhibited higher hydrogen generation rates in the hydrolysis of KBH_4 than that of regular Co–B owing to its larger specific surface area and mesoporous channels. Ma et al. [15] reported the synthesis of hollow Co–B spheres via using polystyrene spheres as sacrificial templates and their excellent catalytic performance for hydrolysis of $NaBH_4$. In addition, Patel et al. [16, 17] discovered that Co–B thin films prepared by pulsed laser deposition have higher catalytic performance in hydrolysis of $NaBH_4$ to produce hydrogen than that of Co–B powders.

Herein, we reported on a novel synthesis strategy for fabricating hollow Co–B nanospindles via using poly(styrene-*co*-methacrylic acid) as templates and their enhanced catalytic performance for hydrolysis of NH_3BH_3 in comparison with that of regular Co–B [12–14] synthesized without using templates.

Experimental

Preparation of hollow Co–B nanospindles

In a typical run of synthesis, poly(styrene-*co*-methacrylic acid) (PSA) nanospindles were prepared through the

D. G. Tong (✉) · X. L. Zeng · D. Wang · P. Wu
College of Materials and Chemistry and Chemical Engineering,
Chengdu University of Technology, Chengdu 610059, China
e-mail: tongdongge@163.com

W. Chu (✉)
Lab 230, College of Chemical Engineering,
Sichuan University, Chengdu 610065, China
e-mail: chuwei65@yahoo.com.cn

emulsifier-free emulsion copolymerization of styrene with methacrylic acid according to a literature procedure [18]. Then, an appropriate amount of the prepared PSA nanoparticles was suspended in distilled water to form a white slurry, and a 0.5 mol/L $Co(OAc)_2$ aqueous solution was added. After the mixture stirred for 30 min, a KBH_4 solution (0.02 mol/L) containing 0.002 mol/L NaOH was added slowly with stirring under argon atmosphere. The obtained composites were dispersed in toluene. The final product was collected by centrifugation, washed with water and ethanol several times, and kept in absolute ethanol until use. The as-prepared Co–B samples were designated as Co–B–*x*, where *x* represents the weight ratio of PSA to $Co(OAc)_2$. The regular Co–B [12–14] was synthesized via a similar process that described above without using PSA nanospindles.

Hydrogen generation and recycle test

The hydrolysis of ammonia borane was according to a procedure reported by the literature [7]. 5 mg catalyst was placed in a three-necked glass container and mixed with 50 mL 0.5 wt% NH_3BH_3 aqueous solution under constant stirring. The generated amount of H_2 was measured via a gas flow meter [13, 14]. After the hydrogen generation reaction was completed, the hollow Co–B nanospindles were magnetically attracted to the bottom of the reaction flask by a magnet, and the upper solution was removed. Then the new NH_3BH_3 aqueous solution (0.5 wt%) was added into the reaction flask. Such recycle experiments were repeated for seven times under ambient atmosphere.

Characterization

Samples were characterized by transmission electron microscopy (TEM, JEOL JSM-200CX), Fourier transform infrared (FTIR, Nicolet 510SX) spectroscopy, inductively coupled plasma optical emission spectrometry (ICP, Irris, Avantage), X-ray powder diffraction using Cu Kα sources (XRD, D/rmax-rA), N_2 adsorption–desorption, X-ray photoelectron spectroscopy (XPS, Perkin-Elmer 5000C ESCA, Al Ka), and magnetic properties (MagLab-12, Oxford). TEM samples were prepared by drying sample droplets from an ethanolic dispersion onto a 300-mesh Cu grid coated with a lacey carbon film.

Results and discussion

As seen in TEM images shown in Fig. 1a, the PSA nanospindles were prepared and well dispersed. The notable different morphologies between the templates and the as-prepared samples (Fig. 1b–d) confirm the formation of Co–B hollow nanospindles regardless of the preparation conditions. The pale color regions in the central parts (Fig. 1b–d) in contrast to the dark edges indicate that the obtained nanospindles exhibit hollow structure with a wall thickness of 4–6 nm. These characteristics endow the

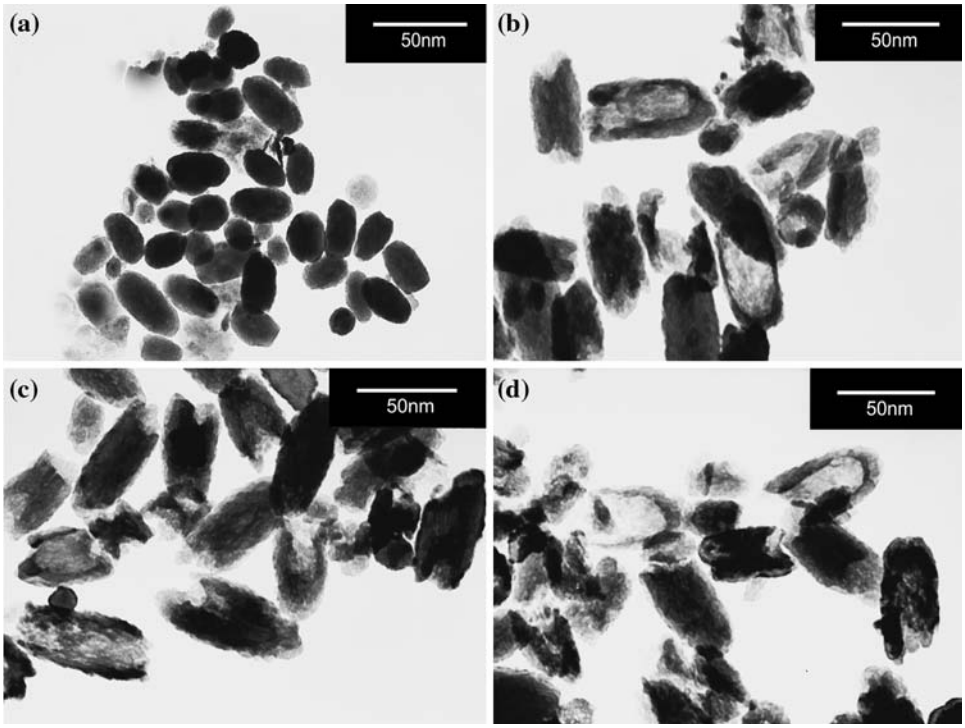

Fig. 1 **a** TEM image of PSA nanospindles; **b** TEM image of Co–B−0.7; **c** TEM image of Co–B−1; **d** TEM image of Co–B−1.5; **e** FTIR spectrum of Co–B−1 hollow nanospindles; **f** XRD pattern of Co–B−1 hollow nanospindles; **g** Schematic formation for Co–B hollow nanospindles

Fig. 1 continued

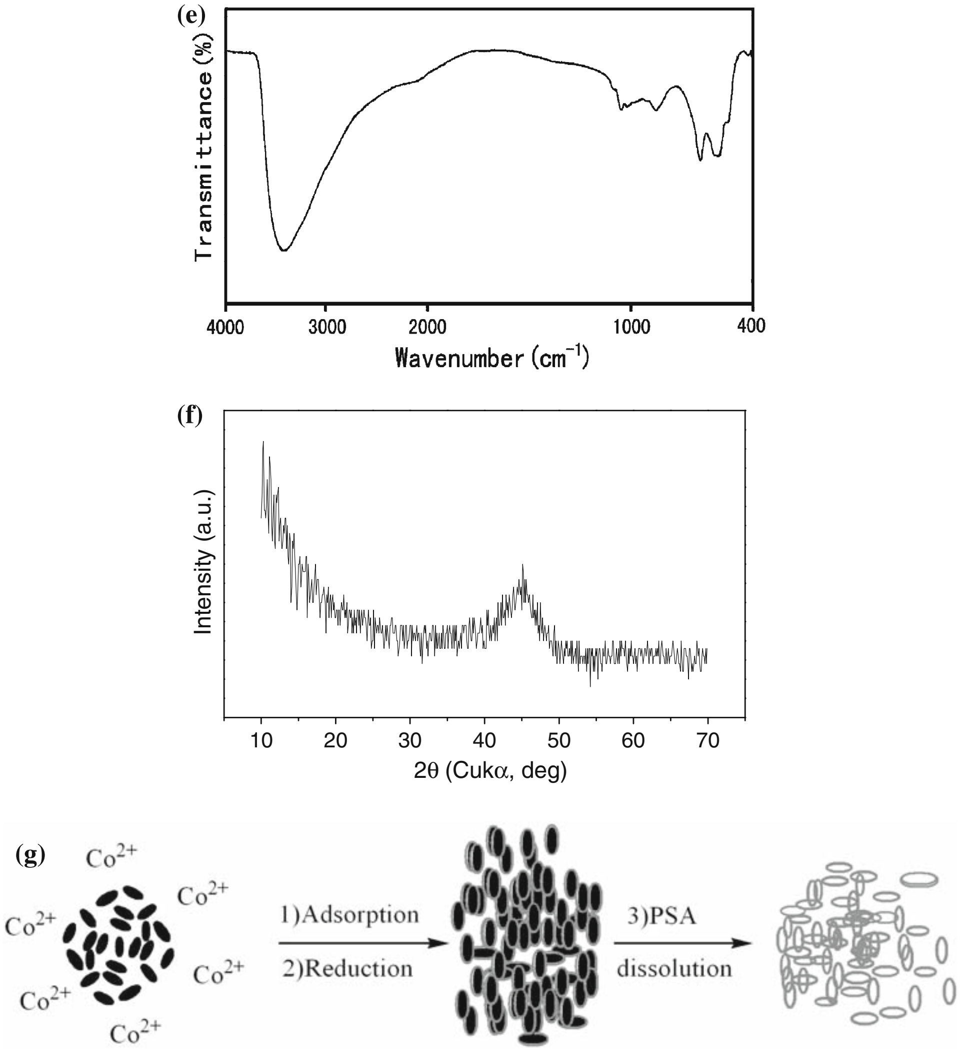

Co–B hollow nanospindles with high specific surface areas (S_{BET}). As shown in Table 1, all of the Co–B hollow nanospindles displayed much larger S_{BET} than the regular Co–B [12–14]. The maximum S_{BET} (143.09 m^2/g) was obtained on Co–B−1.

The FTIR spectrum (Fig. 1e) demonstrates that the Co–B−1 hollow nanospindles show almost the same FTIR spectrum as the regular Co–B [12, 13, 19]. The result indicates that the applied PSA templates had been removed and the formed hollow structure did not affect the vibration behavior of Co–B significantly.

The XRD pattern presented in Fig. 1f shows that, similar to the regular Co–B [12–14], the Co–B−1 hollow nanospindles exhibited a single broad peak around $2\theta = 45.5^\circ$ indicative of amorphous structure [10–15, 19–21]. Meanwhile, the bulk composition (Table 1) of the as-prepared Co–B nanospindles was different with that of the regular Co–B ($Co_{63.0}B_{37.0}$) [12–14], which is attributed to the deviation in the procedures in the preparation of Co–B particles [10, 11].

From above results, the formation of Co–B hollow nanospindles might be illustrated in Fig. 1g. PSA nanospindles were employed as sacrificial templates for the formation of hollow structures. Co–B was deposited on the surface of the PSA nanospindles when Co^{2+} was reduced by KBH$_4$. The resultant Co–B-PSA core–shell structures were dispersed in a toluene solution to dissolve the PSA template cores, resulting in the formation of Co–B hollow nanospindles.

The XPS spectra (Fig. 2) reveal that the Co species in the Co–B−1 sample present in the metallic state with the binding energy 778.1 eV, which is almost the same as those reported [10–15, 19–21]. Meanwhile, the B species present in the elemental state with a binding energy of 188.2 eV, which is positively shifted 1.1 eV in comparison with the pure B (187.1 eV) [10–15, 19–21]. The result also

Table 1 Structural properties and catalytic performances of the as-prepared catalysts

Catalysts	Composition (atom%)	S_{BET} ($m^2\ g^{-1}$)	Wall thickness (nm)	Hydrogen generation rate ($mL\ min^{-1}\ g(catalyst)^{-1}$)
Regular Co–B	$Co_{63.0}B_{37.0}$	65.00	–	475
Co–B−0.7	$Co_{79.3}B_{20.7}$	133.21	4–6	963
Co–B−1	$Co_{79.3}B_{20.7}$	143.09	4–6	1283
Co–B−1.5	$Co_{79.3}B_{20.7}$	138.63	4–6	1020

Reaction conditions: 5 mg Co–B hollow nanospindles, 50 mL 0.5 wt% aqueous NH_3BH_3, $T = 293$ K

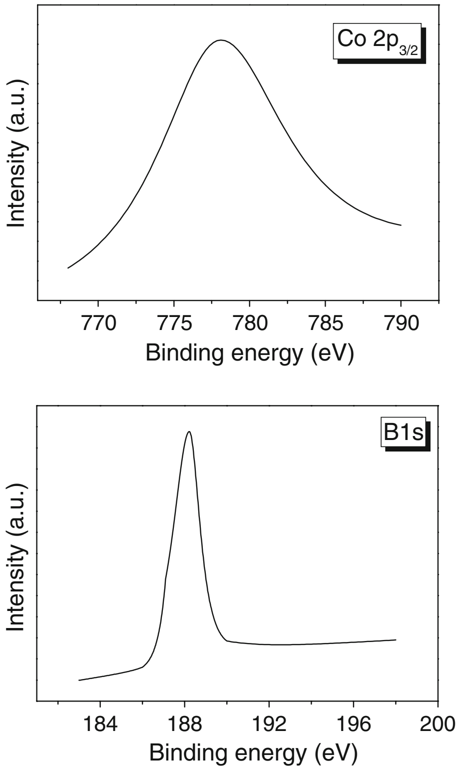

Fig. 2 Co $2p_{3/2}$ and B 1s XPS spectra of Co–B−1 hollow nanospindles

indicates that the elemental B is alloyed with the metallic Co and partial electrons may be transferred from B to Co [10–15, 19–21]. The failure to observe the binding energy shift of the metallic Co could be understood by considering its relatively greater atomic weight compared to that of the B atom [10].

In addition, for Co–B−1 hollow nanospindles, the typical coercivity (H_c), saturation magnetization (M_s), and remanent magnetization (M_r) at 298 K are 243.0 Oe, 42.4 emu/g, and 14.9 emu/g, respectively (Fig. 3). The magnetic properties enable them can be effectively separated by a magnet in a solution system [11–14].

The catalytic hydrolysis of NH_3BH_3 can be expressed as follows:

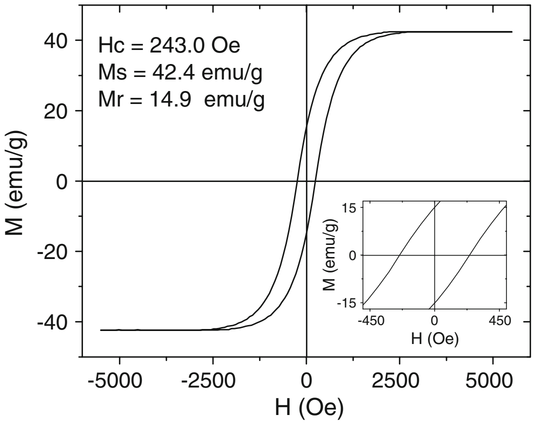

Fig. 3 Hysteresis loops of Co–B−1 hollow nanospindles at room temperature (The *inset* is the full range of the hysteresis measured between −500 and 500 Oe)

$$NH_3BH_3 + 2H_2O \xrightarrow{\text{catalyst}} NH_4^+ + BO_2^- + 3H_2 \uparrow \qquad (1)$$

The Co–B hollow nanospindles exhibited much higher activity than did the regular Co–B (Table 1). The higher activity of Co–B−1 is attributed to its larger specific surface area. From Fig. 4a, it can be seen that the reaction is completed at around 27 min for Co–B−1 hollow nanospindles. After the completion of hydrogen release, the molar ratio of generated H_2 to the initial NH_3BH_3 is close to 3.0, which corresponds to approximately 8.9 wt% of the reactants (i.e., NH_3BH_3 and H_2O, excluding solvent water). According to hydrogen yield, the catalytic performance of the as-synthesized Co–B−1 hollow nanospindles is comparable to that of the reported Pt black [8]. Considering the different price between Pt and Co–B, the Co–B−1 hollow nanospindles are more cost-effective. The favorable activity for the Co–B−1 hollow nanospindles is attributed to their large specific surface area (143.09 m^2/g), which ensures more uniform distribution of the catalytic active sites [12–15], and its hollow structure, which may provide both the inner and the outer surfaces contact between catalysts and NH_3BH_3.

For determining the activation energy, we measured the temperature dependence of hydrogen generation rate using 0.5 wt% aqueous NH_3BH_3 with 5 mg Co–B−1 hollow

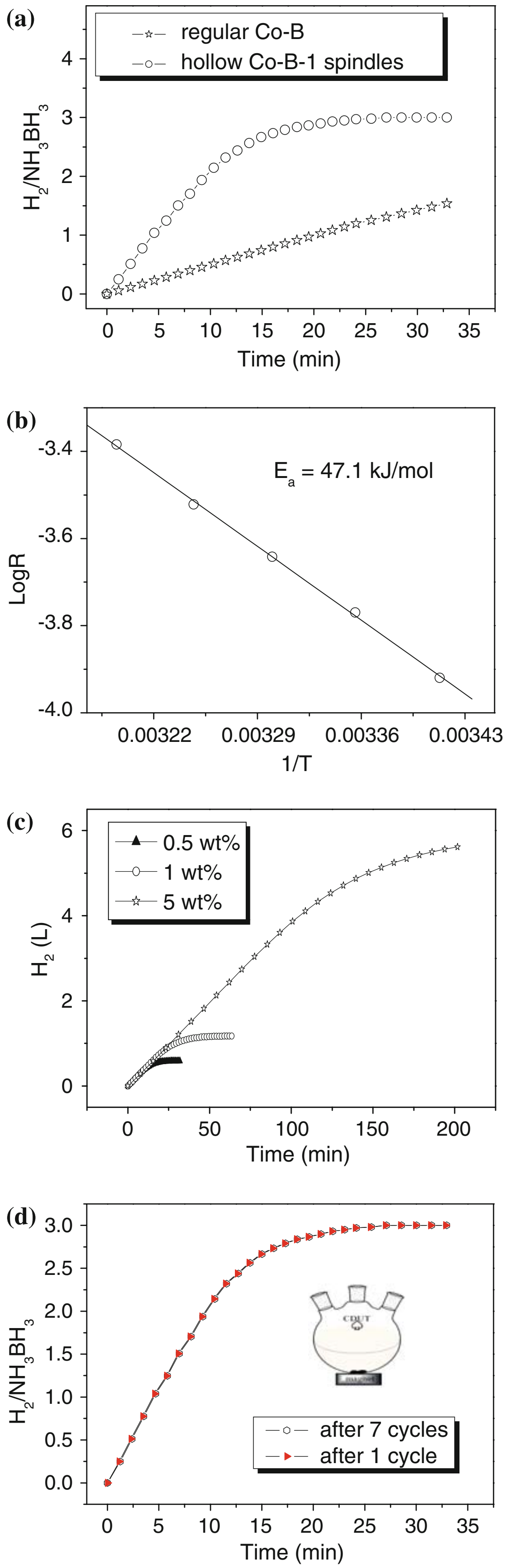

Fig. 4 **a** H_2/NH_3BH_3 molar ratio vs. reaction time of hydrogen ▶ generated from 50 mL 0.5 wt% NH_3BH_3 aqueous solution in the presence of 5 mg Co–B−1 catalysts at 293 K; **b** Plot of log *R* vs. 1/*T* to determine the activation energy of Co–B−1 hollow nanospindles in the reaction (**a**); **c** Hydrogen released from 50 mL aqueous NH_3BH_3 solution with different concentrations in the presence of 5 mg Co–B−1 hollow nanospindles; **d** Cycling performance of Co–B−1 hollow nanospindles in the reaction (**a**)

nanospindles in 20–40 °C. Under our experimental conditions, the reaction rate constant *k* is constant for a given temperature, implying zero order kinetics for the NH_3BH_3 hydrolysis reaction [7, 8, 22]. It suggests that the hydrogen generation rate is controlled within a surface reaction [7, 8, 22]. Thus, the hydrogen generation rate (*R*) can be given as

$$R = k[NH_3BH_3]^0 \tag{2}$$

Through the Arrhenius treatment of the temperature-dependent reaction rates [7, 8, 22], the activation energy (E_a) is determined to be 47.1 kJ mol^{-1} (Fig. 4b).

In addition, we have also investigated the effect of NH_3BH_3 concentration on the hydrolysis reaction in the presence of Co–B−1 hollow nanospindles. As shown in Fig. 4c, the concentration of NH_3BH_3 has some slight influence on the rate of hydrogen generation. In the hydrolysis process of 5% NH_3BH_3 solution, the H_2 release rate slows down during the last period. This rate drop may be due to the blocking of catalyst sites by the formed boracic precipitate in a more concentrated NH_3BH_3 solution [6].

Reusability of Co–B−1 hollow nanospindles was also studied. In our present case, after reaction, the magnetic Co–B−1 hollow nanospindles can be effectively separated by a magnet (Fig. 4d). The easy magnetic separation is greatly useful for the recycle application of Co–B−1 catalyst in a solution system [11–15]. After seven cycles, the activity of Co–B−1 hollow nanospindles has no obvious decrease (Fig. 4d).

Conclusions

In conclusion, Co–B hollow nanospindles have been prepared by a novel and facile method. During the preparation, PSA nanospindles were used as scarified templates, and followed by the removal of PSA via adding toluene. In the hydrolysis of NH_3BH_3 to release H_2, Co–B−1 exhibited higher activity due to its large specific surface areas. Furthermore, its catalytic performance is comparable to that of the reported Pt black concerning hydrogen yield. In addition, Co–B−1 hollow nanospindles have good reusability in the application. After seven cycles, the activity has no obvious decrease.

Acknowledgements This work was supported by Research Funds of CDUT (2007-YG2 and HZ0033), and the Natural Science Foundation of Sichuan Province (07ZA004).

References

1. Sahaym U, Norton MG (2008) J Mater Sci 43:5395. doi:10.1007/s10853-008-2749-0
2. Huang HX, Huang KL, Liu SQ, Zhuang SX, Chen DY (2009) J Mater Sci 44:4460. doi:10.1007/s10853-009-3676-4
3. Holladay JD, Wang Y, Jones E (2004) Chem Rev 104:4767
4. Graetz J (2009) Chem Soc Rev 38:73
5. Wang J, Ebner AD, Ritter JA (2006) J Am Chem Soc 128:5949
6. Cheng FY, Ma H, Li YM, Chen J (2007) Inorg Chem 46:788
7. Xu Q, Chandra M (2006) J Power Sources 156:364
8. Chandra M, Xu Q (2007) J Power Sources 168:135
9. Yan J, Zhang X, Han S, Shioyama H, Xu Q (2008) Angew Chem Int Ed 47:2287
10. Li HX, Chen XF, Wang YP, Xu YP (2002) Appl Catal A Gen 225:117
11. Tong DG, Chu W, Luo YY, Ji XY, He Y (2007) J Mol Catal A Chem 265:195
12. Tong DG, Chu W, Luo YY, Chen H, Ji XY (2007) J Mol Catal A Chem 269:149
13. Tong DG, Han X, Chu W, Chen H, Ji XY (2008) Mater Res Bull 43:1327
14. Tong DG, Han X, Chu W, Chen H, Ji XY (2007) Mater Lett 61:4679
15. Ma H, Ji WQ, Zhao JZ, Chen J (2008) J Alloys Compd 474:584
16. Patel N, Guella G, Kale A, Miotello A, Patton B, Zanchetta C, Mirenghi L, Rotolo P (2007) Appl Catal A Gen 323:18
17. Patel N, Fernandes R, Guella G, Kale A, Miotello A, Patton B, Zanchetta C (2008) J Phys Chem C 112:6968
18. Caruso F, Caruso RA, Mohwald H (1998) Science 282:1111
19. Tong DG, Chu W, Zeng XL, Tian W, Wan D (2009) Mater Lett 63:1555
20. Tong DG, Hu JY, Chu W, Zhang T, Ji XY (2008) Mater Lett 62:2746
21. Tong DG, Luo YY, Chu W (2008) Mater Chem Phys 112:907
22. Guo XH (2003) Kinetics for applied chemical engineering. Chemistry Industry Publishing House, Beijing